Flexural Vibration of Timoshenko Beams, Using Distributed Lumped Modeling Technique

A. Farshidianfar[1], S. Soheili,[2] and M. Abachizadeh[3]
Mech. Eng. Dep't., Ferdowsi Univ. of Mashhad

ABSTRACT
This paper focuses on the development of a complete model of the Timoshenko beam, based on considering the effects of shear deformation. A method based on distributed-lumped modeling approach is proposed to solve the governing equations. Natural frequencies obtained by this method are compared and verified with Chebyshev pseudospectral method. The effects of shear deformation on natural frequency of pinned and clamped beams are discussed for various diameters. In addition, the effects of lumped mass and its position are investigated for clamped and pinned rotors with different diameters. It is shown that, while the new method leads to highly accurate results, its simplicity and accuracy makes it appropriate for application on industrial systems.

Key Words: Distributed Lumped Modeling, Timoshenko Beam Theory, Shear Deformation

بررسی ارتعاشات عرضی تیر تیموشنکو با استفاده از روش مدلسازی گسترده- متمرکز

انوشیروان فرشیدیانفر، سعید سهیلی و مهدی عباچی زاده
گروه مهندسی مکانیک، دانشگاه فردوسی مشهد

(تاریخ دریافت: ۱۳۸۶/۱/۲۱؛ تاریخ پذیرش: ۱۳۸۷/۰۳/۲۷)

چکیده
این مقاله به بررسی مدل کامل تیر تیموشنکو بر اساس آثار تغییر شکل برشی می‌پردازد. برای حل معادلات حاکم، روشی بر اساس نظریه مدل‌سازی با المان‌های گسترده- متمرکز پیشنهاد شده است. فرکانس‌های طبیعی بدست آمده از این روش با نتایج روش چند جمله ای‌های چبیشف مقایسه و تأیید شده است. تأثیر تغییر شکل برشی بر فرکانس‌های طبیعی تیر دوسر ساده و دوسر گیردار برای قطرهای مختلف مورد بحث قرار گرفته است. بعلاوه، اثر جرم متمرکز و موقعیت آن برای روتورهای دوسر ساده و دوسر گیردار با قطرهای متفاوت بررسی شده است. در حالی که روش جدید به نتایج کاملاً دقیقی منجر می‌شود، سادگی و دقت بالا آن را برای به‌کارگیری در سیستم‌های صنعتی مناسب می‌سازد.

واژه‌های کلیدی: مدلسازی گسترده، متمرکز، تئوری تیر تیموشنکو، تغییر شکل برشی

1-Associate Professor (Corresponding Author): farshid@ferdowsi.um.ac.ir
2- PhD Student: sa_so107@stu-mail.um.ac.ir
3- MSc. Student: m_abachizadeh@yahoo.com

1- Introduction

The effects of shear deformation on the vibration and natural frequencies of thick beams have been investigated since long before. The frequencies of Euler-Bernoulli beam theory is considered in many articles and vibration textbooks, such as [1]. The vibration equations consisting shear effects were presented by Timoshenko [2] for the first time, and many efforts have been performed to solve the Timoshenko differential equation of vibration.

Generally speaking, there are three types of solutions for this equation. Firstly, some analytical solutions are presented for very restricted cases and limited boundary conditions [2-4]. Secondly, the semi-analytic solutions are proposed for this problem such as differential quadrature method [5], the boundary characteristic orthogonal polynomials [6] and the Chebyshev pseudospectral method [7]. Finally, there are some numerical and approximate methods such as finite element and finite difference method. However, no general analytical and exact solution is provided for Timoshenko beam equation.

The distributed-lumped modeling technique (DLMT) was introduced by Whalley [8] for the first time. This technique was applied by Aleyaasin et al. [9] for calculating the flexural frequencies of shafts using 4*4 matrices. Aleyaasin and Ebrahimi also obtained the frequency response of such systems [10]. Further investigations about the flexural vibration of rotor bearing systems was performed by Aleyaasin et al., see for example references [11] and [12]. The distributed-lumped method also can be applied to other systems, such as modeling the torsional [13] and longitudinal vibration and calculating frequency and time responses in forced systems [14]. It can also be applied to the fluid systems, as represented by Whalley et al [15].

In this paper, the flexural vibration of a Timoshenko beam is analyzed via distributed-lumped modeling technique (DLMT). To verify the accuracy of present method, the results obtained by this hybrid modeling technique (DLMT) are compared with the results of Lee and Schultz [7]. The effect of beam thickness, disk mass and its position on the first natural frequency is investigated for clamped and pinned boundary conditions, and compared with the Euler-Bernoulli beam theory.

2. The General Distributed-lumped Model

Generally speaking, systems in the hybrid modeling technique are considered as the combination of two types of element:

1) The distributed element, which is the main part of shafts and rotors; with the distributed mass or inertia and
2) The lumped element, which is the supplementary part of shafts and rotors; with the concentrated mass or inertia such as disks, gears, propellers, pulleys, and so on.

In this way, the final vibration model of system is obtained by setting the distributed and lumped matrices of different parts and combining them together. Distributed and lumped matrices are formed based on the analytical equations of motion, so this is the highly accurate technique in contrast with the other approximate techniques such as the transfer matrix method (based on lumped elements), finite element method, and so on. Another advantage of this technique, compared with analytical method, is that the continuity conditions between elements are simply satisfied and it remains only to apply the boundary conditions of the system to the model.

2.1- Transfer Matrix of Distributed Element

According to Fig. **1**, the Timoshenko beam equation for a thick beam with the density ρ, modulus of elasticity E and shear modulus G can be expressed as 1:

$$EI\frac{\partial^4 y}{\partial x^4} - \rho A\omega^2 y + (\rho I + \frac{\rho EI}{kG})\omega^2 \frac{\partial^2 y}{\partial x^2} + \frac{\rho^2 I}{kG}\omega^4 y = 0 \quad . \tag{1}$$

In this equation, I denotes the area moment of inertia and A is the cross sectional area of beam, while k denotes the shear coefficient and ω is the frequency of vibration. As it is clear from the latter terms, this equation is consisting shear deformation and rotary inertia effects.

In order to solve Eq. (1), y is assumed to be the function of x and ω in the following form:

$$y(x,\omega) = ce^{nx} \quad . \tag{2}$$

In this equation, n is a frequency dependent function, and c is a constant calculated according to the boundary conditions. It is clear that there is no approximation in this solution, while it includes all of the sinusoidal functions as well. It can be easily applied to find other parameters. Substitution of this equation in Eq. (1) gives:

$$n^4 + an^2 + b = 0, \tag{3}$$

in which, a and b are frequency dependent terms as follows:

$$a = (\frac{1}{E} + \frac{1}{kG})\rho\omega^2 \quad , \tag{4}$$

$$b = (-\frac{A}{EI} + \frac{\rho}{kGE}\omega^2)\rho\omega^2 \quad . \tag{5}$$

Therefore, n is obtained by solving Eq. (3) as the following form:

$$n = \pm\sqrt{\frac{-a \pm \sqrt{a^2 - 4b}}{2}} \quad . \tag{6}$$

In this way, 4 quantities are obtained for *n*, hence, $y(x,\omega)$ can be expressed as follows:

$$y = \sum_{i=1}^{4} c_i e^{(n_i x)} \quad . \tag{7}$$

The shear force *V*, slope function θ and bending moment *M* should be stated by the geometry and material parameters (independent of each other).

In order to obtain the The shear force *V*, momentum equation for *dx* element is to be written in the following form (see Fig. **1**):

$$\frac{\partial M}{\partial x} - V = -\rho I \omega^2 \theta \ . \tag{8}$$

According to Timoshenko beam theory, the slope is the function of deflection and shear force as follows:

$$\theta = \frac{\partial y}{\partial x} + \frac{V}{kAG} \quad . \tag{9}$$

Another relation is obtained by recalling mechanics of materials:

$$M = EI \frac{\partial \theta}{\partial x} \ , \tag{10}$$

and force equation could be stated as follows:

$$\frac{\partial V}{\partial x} = -\rho A \omega^2 y \ . \tag{11}$$

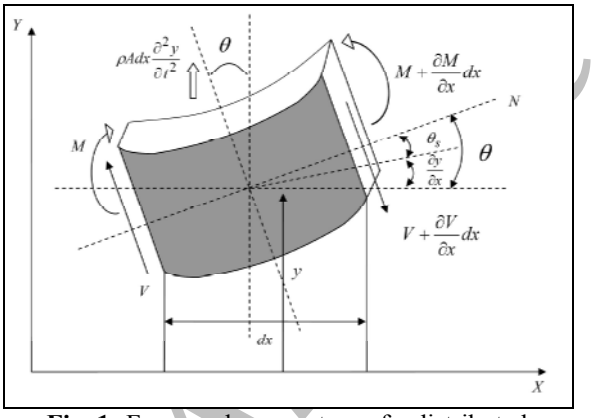

Fig. 1: Force and momentum of a distributed element.

Substitution of Eqs. (9), (10) in Eq. (8) would result in:

$$EI \frac{\partial^3 y}{\partial x^3} + \frac{EI}{kAG} \frac{\partial^2 V}{\partial x^2} - V = -\rho I \omega^2 \frac{\partial y}{\partial x} - \frac{\rho I}{kAG} \omega^2 V. \tag{12}$$

The shear force *V* can be obtained by the substitution of Eq. 11 into 12. The result can be stated as:

$$V = (kAG)\left(EI \frac{\partial^3 y}{\partial x^3} + \rho I (1 + \frac{E}{kG}) \omega^2 \frac{\partial y}{\partial x} \right) \Big/ \left(kAG - \rho I \omega^2 \right). \tag{13}$$

Substituting this relation in Eqs. 9 and 10 gives:

$$\theta = \frac{\partial y}{\partial x} + \left(EI \frac{\partial^3 y}{\partial x^3} + \rho I (1 + \frac{E}{kG}) \omega^2 \frac{\partial y}{\partial x} \right) \Big/ \left(kAG - \rho I \omega^2 \right), \tag{14}$$

$$M = EI \frac{\partial^2 y}{\partial x^2} + EI \left(EI \frac{\partial^4 y}{\partial x^4} + \rho I (1 + \frac{E}{kG}) \omega^2 \frac{\partial^2 y}{\partial x^2} \right) \Big/ \left(kAG - \rho I \omega^2 \right). \tag{15}$$

Since in Eq. 7, n_i is independent of *x*, differentiating *y* with respect to *x* in this equation yields:

$$\frac{\partial^m y}{\partial x^m} = \sum_{i=1}^{4} c_i (n_i)^m e^{(n_i x)} \ , \tag{16}$$

where, *m*=1, 2, 3, 4. Equations (7), (13), (14) and (15) can be written in the matrix form as:

$$\begin{Bmatrix} y \\ \theta \\ M \\ V \end{Bmatrix} = [\mathbf{T}(x)]\{C\} \ , \tag{17}$$

where, $[\mathrm{T}(x)]$ and $\{C\}$ are the transfer matrix and the coefficient vector, respectively. For the simple representation of transfer matrix $[\mathrm{T}(x)]$, one can assume that:

$$y_i = e^{(n_i x)}, \quad i = 1, 2, 3, 4 \ . \tag{18}$$

The parameters θ_i, M_i and V_i are obtained by the substitution of y_i and its differentials in Eq's. (14), (15) and (13), respectively. Therefore, the transfer matrix $[\mathrm{T}(x)]$ can be stated as:

$$[\mathbf{T}(x)] = \begin{bmatrix} T_{11} & T_{12} & T_{13} & T_{14} \\ T_{21} & T_{22} & T_{23} & T_{24} \\ T_{31} & T_{32} & T_{33} & T_{34} \\ T_{41} & T_{42} & T_{43} & T_{44} \end{bmatrix}, \tag{19a}$$

where,

$$T_{1i} = y_i, \ T_{2i} = \theta_i, \ T_{3i} = M_i, \ T_{4i} = -V_i \ , \tag{19b}$$

and $\{C\}$ is the coefficient vector as:

$$\{C\} = \begin{Bmatrix} c_1 \\ c_2 \\ c_3 \\ c_4 \end{Bmatrix} \quad . \tag{20}$$

The minus sign in Eq. (19b) is considered to change the *V* direction to the positive direction of *y*.

Ignoring rotary inertia and shear deformation effects, the transfer matrix components based on the Euler-Bernoulli beam theory and its solution using the above method are presented in Ref. [16].

Considering a beam with *n* elements and focusing our attention on *j*th element, for the initial point of

shaft (for example, the left side of it), one should assign *x=0* in Eq. (17), as:

Shaft (for example the left side of it), one shoud assign x=0 in Eq. 17, as:

$$\begin{Bmatrix} y(0) \\ \theta(0) \\ M(0) \\ V(0) \end{Bmatrix}_j = [\mathbf{T}(0)]_j \{C\}_j \ . \tag{21}$$

Therefore, the coefficient vector can be expressed as:

$$\{C\}_j = [\mathbf{T}(0)]_j^{-1} \begin{Bmatrix} y(0) \\ \theta(0) \\ M(0) \\ V(0) \end{Bmatrix}_j \ . \tag{22}$$

For the shaft element with length *l*, assuming *x=l* gives:

$$\begin{Bmatrix} y(l) \\ \theta(l) \\ M(l) \\ V(l) \end{Bmatrix}_j = [\mathbf{T}(l)]_j [\mathbf{C}]_j \ . \tag{23}$$

Substituting Eq's. (22) into (23) and applying the continuity equation as:

$$\begin{Bmatrix} y(0) \\ \theta(0) \\ M(0) \\ V(0) \end{Bmatrix}_j = \begin{Bmatrix} y \\ \theta \\ M \\ V \end{Bmatrix}_{j-1} , \tag{24}$$

would result in:

$$\begin{Bmatrix} y \\ \theta \\ M \\ V \end{Bmatrix}_j = [\mathbf{T}_D]_j \begin{Bmatrix} y \\ \theta \\ M \\ V \end{Bmatrix}_{j-1} , \tag{25}$$

where ,

$$[\mathrm{T}_D]_j = [\mathrm{T}(l)]_j [\mathrm{T}(0)]_j^{-1} , \tag{26}$$

where $[\mathrm{T}_D]$ is the main transfer matrix for the distributed element in DLMT, where the components of it are presented in Appendix A.

2.2- Transfer Matrix of Lumped Element

According to Fig's. **2** and 3, the relationship between the right and left side of *j*th lumped element such as a gear, pulley, and so on, regarding rotary inertia and gyroscopic effects, can be expressed as follows:

$$\begin{aligned} y_j &= y_{j-1}, \\ \theta_j &= \theta_{j-1}, \\ M_j &= M_{j-1}, \\ V_j &= V_{j-1} - m_d \omega^2 y, \end{aligned} \tag{27}$$

which can be expressed in the matrix form as:

$$\begin{Bmatrix} y \\ \theta \\ M \\ V \end{Bmatrix}_j = [\mathbf{T}_L]_j \begin{Bmatrix} y \\ \theta \\ M \\ V \end{Bmatrix}_{j-1} , \tag{28}$$

where,

$$[\mathbf{T}_L]_j = \begin{bmatrix} 1 & 0 & 0 & 0 \\ 0 & 1 & 0 & 0 \\ 0 & 1 & 1 & 0 \\ -m_d\omega^2 & 0 & 0 & 1 \end{bmatrix} . \tag{29}$$

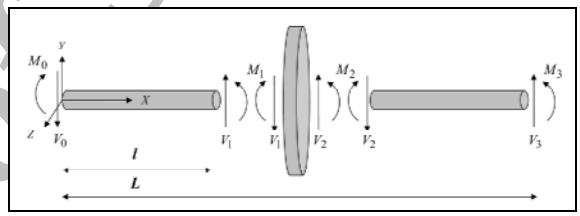

Fig. (2): General model of vibrating shaft system.

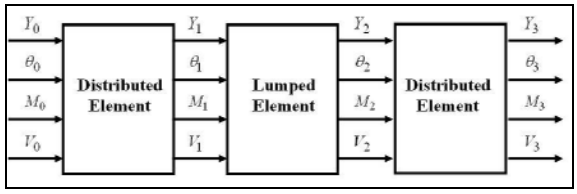

Fig. (3): Hybrid model of vibrating shaft system.

3. Numerical Results and Discussions

In this section, the methodology outlined previously is applied to the shaft with two different boundary conditions; pinned-pinned (P-P) and clamped-clamped (C-C), which is a simplified model for common industrial and structural systems. The results are compared and verified with the results of Chebyshev pseudospectral method obtained by Lee et al. [7] for different thickness-to-length ratios (h/l= 0.002, 0.02, 0.2). In addition, the relative changes of the first natural frequency for different thickness-to-length ratios (h/l= 0.001 to 0.5) are plotted for these commonest boundary conditions. The effects of shear deformation, shaft thickness, disk mass and its position on the first natural frequency are investigated. The properties of the systems considered here are presented in Tables (**1**) and (**2**).

Table 1: Properties of the beam.

Beam Length l	1 m
Beam Width b	0.1 m
Beam Thickness h	0.002, 0.02, 0.2 m
Density of Shaft Material ρ	7800 kg/m^3
Modulus of Elasticity for Shaft E	200 GPa
Poisson Ratio v	0.30
Shear Coefficient k	5/6

Table 2: Properties of the rotor.

Shaft Length L	1 m
Shaft Diameter d_{shaft}	0.02, 0.2 m
Density of Shaft Material ρ	7800 kg/m^3
Modulus of Elasticity for Shaft E	200 GPa
Poisson Ratio v	0.30
Mass of Disk	0-1000 kg
Disk Position l	0.1, 0.3, 0.5 m
Shear Coefficient k	9/10

These examples verify the results of the new method and approve the accuracy of them as well. They also show the simplicity of formulation for modeling of structural and industrial systems with any boundary conditions. As it was already mentioned, the present method can be used for analyzing systems with any number of distributed and lumped elements without increasing in difficulty. It can be also applied on shafts with different sections just by setting the distributed matrices for each section and multiplying them.

3.1. Verification of the Results

The distributed-lumped modeling technique can be simply applied to various types of boundary conditions. In order to verify the proposed methodology, this technique is used to obtain the natural frequencies of different boundary conditions such as C-C and P-P. These conditions are applied as follows.

Firstly, the Eq. (25) should be expanded into 4 equations as:

$$y_1 = T_{11}y_0 + T_{12}\theta_0 + T_{13}M_0 + T_{14}V_0 \quad , \tag{30}$$

$$\theta_1 = T_{21}y_0 + T_{22}\theta_0 + T_{23}M_0 + T_{24}V_0 \quad , \tag{31}$$

$$M_1 = T_{31}y_0 + T_{32}\theta_0 + T_{33}M_0 + T_{34}V_0 \quad , \tag{32}$$

$$V_1 = T_{41}y_0 + T_{42}\theta_0 + T_{43}M_0 + T_{44}V_0 \quad . \tag{33}$$

(a) C-C shaft: based on the boundary conditions, state vector in this case can be expressed as: $\{Z\}_0 = \{0 \;\; 0 \;\; M_0 \;\; V_0\}$, $\{Z\}_1 = \{0 \;\; 0 \;\; M_1 \;\; V_1\}$. Hence, in this case, Eqs. 30 and 31 can be rearranged as follows:

$$T_{13}M_0 + T_{14}V_0 = 0 \quad , \tag{34}$$

$$T_{23}M_0 + T_{24}V_0 = 0 \quad . \tag{35}$$

For the nontrivial solution of the simultaneous homogeneous equations, the determinant of coefficients of M_0 and V_0 should vanish, that is:

$$\det\begin{bmatrix} T_{13} & T_{14} \\ T_{23} & T_{24} \end{bmatrix} = 0 \quad . \tag{36}$$

Equation (36) is the frequency equation for the assumed model, since the natural frequencies are obtained by solving this equation.

(b) P-P shaft: based on the boundary conditions, state vector in this case can be expressed as: $\{Z\}_0 = \{0 \;\; \theta_0 \;\; 0 \;\; V_0\}$, $\{Z\}_1 = \{0 \;\; \theta_1 \;\; 0 \;\; V_1\}$. Substitution of this relation in Eqs. 30 and 32 results in the characteristic equation for the P-P shaft as follows:

$$\det\begin{bmatrix} T_{12} & T_{14} \\ T_{32} & T_{34} \end{bmatrix} = 0 \quad . \tag{37}$$

Tables **3** and **4** present the results obtained by DLMT for the shafts with *h/l*= 0.002, 0.02, 0.2 based on C-C and P-P boundary conditions, respectively; where *h* is the beam thickness and *h=2r* in circular cross sections. These frequencies are compared and verified in the mentioned tables with the results of Chebyshev pseudo spectral method obtained by Lee et al. [7], which show a very good agreement with them. The result shown in these tables are non-dimensionalized frequencies calculated as follows:

$$\lambda_i^2 = \omega_i l^2 \sqrt{\frac{\rho A}{EI}} \quad . \tag{38}$$

The calculations show that the error of Chebyshev pseudo spectral method in respect to DLMT is less than 0.03% for the C-C shaft; and less than 0.1% for the P-P boundary conditions, which approves the accuracy of the DLMT method.

The Euler-Bernoulli beam theory results as a classical method obtained by DLMT are also presented in the mentioned tables for both cases. As it is expected, the frequencies calculated by using the classical and Timoshenko beam theory are highly close together in the lower *h/l* ratios, while they are completely different in the higher *h/l* ratios. Actually, there are some extra frequencies in thick shafts which are neglected in the classical beam

theory, and only Timoshenko theory can predict them.

3.2. The Effect of Shaft Diameter

In order to investigate the effect of shaft thickness on its natural frequency, simply supported and clamped shafts with different thicknesses are considered. The first natural frequency for these shafts are calculated according to change in the thickness-to-length ratio (h/l= 0.001 to 0.5) for rectangular or circular cross sections, and the results are shown in Fig. **4.**

According to this figure, the clamped beam shows 31% decline in the first natural frequency (λ_1) for the rectangular (k=5/6) cross sections, while the decline for the pinned one is nearly 13% in the maximum thickness.

It is clear that more restricted boundary conditions leads to higher decline in the first natural frequency (λ_1) by increasing the shaft thickness. However, the Euler-Bernoulli beam theory shows nearly no changes in λ_1 in any case.

3.3. The Effect of Disk

In this section, the application of DLMT on more complicated systems is investigated. It can be seen that how the distributed-lumped technique can be easily applied to calculate any natural frequency of highly complicated systems with any number of distributed and lumped elements and how it brings highly accurate results.

In order to illustrate the effects of disk mass and its position on the natural frequencies of rotors, a rotor with only one disk (lumped mass) is studied with pinned boundary condition, which is more common in real systems. The rotor's radius is assumed as r=0.01, 0.1m and the disk position is considered as l/L=0.1, 0.3, 0.5 for a shaft (circular cross section, k=9/10) with 1m length.

To represent the main hybrid model of the system, it should be noticed that the system is combined with two distributed and one lumped elements Fig. **3**. For the distributed elements 1 and 3 the transfer matrices can be written according to Eq. (25) as:

$$\begin{Bmatrix} y_1 \\ \theta_1 \\ M_1 \\ V_1 \end{Bmatrix} = [T_D]_1 \begin{Bmatrix} y_0 \\ \theta_0 \\ M_0 \\ V_0 \end{Bmatrix}, \begin{Bmatrix} y_3 \\ \theta_3 \\ M_3 \\ V_3 \end{Bmatrix} = [T_D]_3 \begin{Bmatrix} y_2 \\ \theta_2 \\ M_2 \\ V_2 \end{Bmatrix}, \quad (39)$$

where,

$$[T_D]_j = [T(l)]_j [T(0)]_j^{-1} \quad , \quad (40)$$

and for the lumped element there will be:

$$\begin{Bmatrix} y_2 \\ \theta_2 \\ M_2 \\ V_2 \end{Bmatrix} = [T_L]_2 \begin{Bmatrix} y_1 \\ \theta_1 \\ M_1 \\ V_1 \end{Bmatrix} \quad , \quad (41)$$

Substituting Eq's. (41) into (39) yields:

$$\begin{Bmatrix} y_3 \\ \theta_3 \\ M_3 \\ V_3 \end{Bmatrix} = [T] \begin{Bmatrix} y_0 \\ \theta_0 \\ M_0 \\ V_0 \end{Bmatrix} \quad , \quad (42)$$

where,

$$[T] = [T_D]_3 [T_L]_2 [T_D]_1 \quad . \quad (43)$$

Equation (42) is the main equation for flexural vibration of the system which relates left and right ends of the system.

Figures **5** and **6** show the results for the P-P rotor with r=0.01, 0.1m, respectively. In the figures, the percentage of relative change in the first natural frequency, $(\omega - \omega_0)/\omega_0 \times 100$, is plotted versus the disk mass (m_d = 0-1000 kg). As it is expected, the frequency shows more decrease by increasing the disk mass for the rotor with smaller diameter.

The results also show more decline in the first natural frequency by increasing the disk mass for the disks closer to the middle of the rotor. Actually, the disk positions l/L=0.3, 0.5 show more decline in the frequency and their decline quantities in both figures are closer together, while the position l/L=0.1 shows less decrease and its quantities are absolutely higher than the other positions. According to Fig. **5**, it can be seen that increasing the disk mass up to nearly 100kg brings nearly 90 percent decrease in the amount of frequency for l/L=0.3, 0.5, while it is 80 percent for 200kg disk mass. More increasing the disk mass shows very few changes in the frequency.

4. Conclusions

In this paper, a new solution for the Timoshenko beam equation is presented. Combined with distributed-lumped modeling technique, it brings a highly accurate model of vibrating systems. The results obtained by this method are compared with Lee and Schultz [7] results for various boundary conditions, and good conformity is achieved. The effect of beam thickness, disk mass and its position on the first natural frequency is investigated for

clamped and pinned (C-C and P-P) rotors. The total decline of λ_i for various thickness ratios of beams is studied. It is shown that the shaft with more restricted boundary conditions shows more decline in the first natural frequency by increasing the thickness. It is also shown that closer disk to the middle of rotor brings more decline in natural frequencies.

Table 3: The comparison of natural frequencies using the DLMT and the pseudospectral method for C-C shaft.

Mode No.	Classical Theory	*h/l*= 0.002		*h/l*= 0.02		*h/l*= 0.2	
		Present Method	Lee and Schultz [2]	Present Method	Lee and Schultz [2]	Present Method	Lee and Schultz [2]
1	4.7300404531	4.7299750076	4.72998	4.7232057299	4.72350	4.2420125440	4.24201
2	7.8532044883	7.8509797784	7.85295	7.8281714212	7.82817	6.4179365061	6.41794
3	10.994607704	10.994983051	10.9950	10.934115990	10.9341	8.2853167355	8.28532
4	14.136022955	14.134813042	14.1359	14.015425157	14.0154	9.9037211976	9.90372
5	17.278759576	17.276573252	17.2766	17.067780178	17.0679	11.348744396	11.3487
6	20.419651146	20.416300642	20.4168	20.086796613	20.0868	12.640244949	12.6402
7	23.561946198	23.556683501	23.5567	23.068118989	23.0682	13.456738980	13.4567
8	26.702863279	26.696049952	26.6960	26.008606177	26.0086	13.810137261	13.8101
9	29.844968384	29.835224673	29.8348	28.905184798	28.9052	14.480557252	14.4806
10	32.984082317	32.973191671	32.9729	31.755991198	31.7558	14.938292031	14.9383

Table 4: The comparison of natural frequencies using the DLMT and the pseudospectral method for P-P shaft.

Mode No.	Classical Theory	*h/l*= 0.002		*h/l*= 0.02		*h/l*= 0.2	
		Present Method	Lee and Schultz [2]	Present Method	Lee and Schultz [2]	Present Method	Lee and Schultz [2]
1	3.1386487017	3.1386487017	3.14158	3.1405008298	3.14053	3.0453306363	3.04533
2	6.2831850577	6.2831001317	6.28310	6.2746813177	6.27471	5.6715511345	5.67155
3	9.4232086948	9.4232086948	9.42449	9.3963090742	9.39632	7.8395173454	7.83952
4	12.565488166	12.565689332	12.5657	12.499397265	12.4994	9.6570915656	9.65709
5	15.707404630	15.706632851	15.7066	15.578404324	15.5784	11.222039287	11.2220
6	18.849555899	18.846417389	18.8473	18.628231865	18.6282	12.602210880	12.6022
7	21.991148790	21.986881963	21.9875	21.644305550	21.6443	13.032326963	13.0323
8	25.132337376	25.126892762	25.1273	24.622664891	24.6227	13.444274238	13.4443
9	28.273860645	28.266687894	28.2666	27.559948783	27.5599	13.843285665	13.8433
10	31.412903703	31.405280425	31.4053	30.453648939	30.4533	14.437763890	14.4378

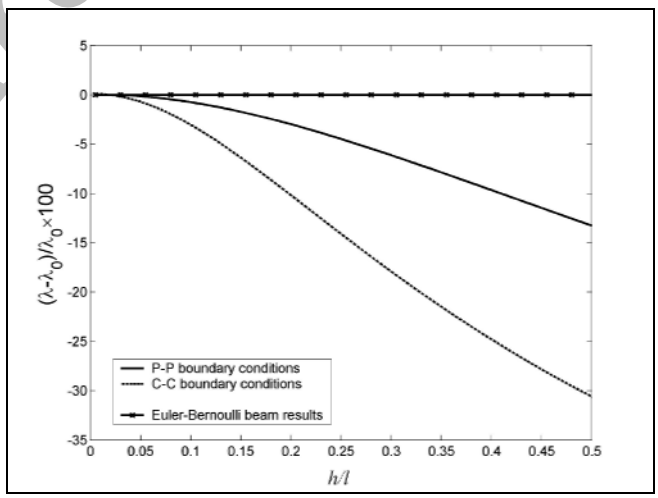

Fig. 4: DLMT solution: Relative change of the first natural frequency vs. beam thickness.

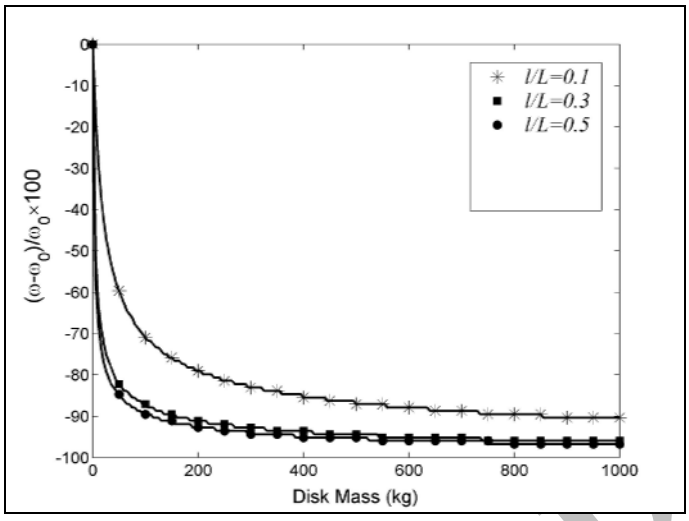

Fig. 5: Relative change of the first natural frequency vs. disk mass for a P-P shaft (with r=0.01 m).

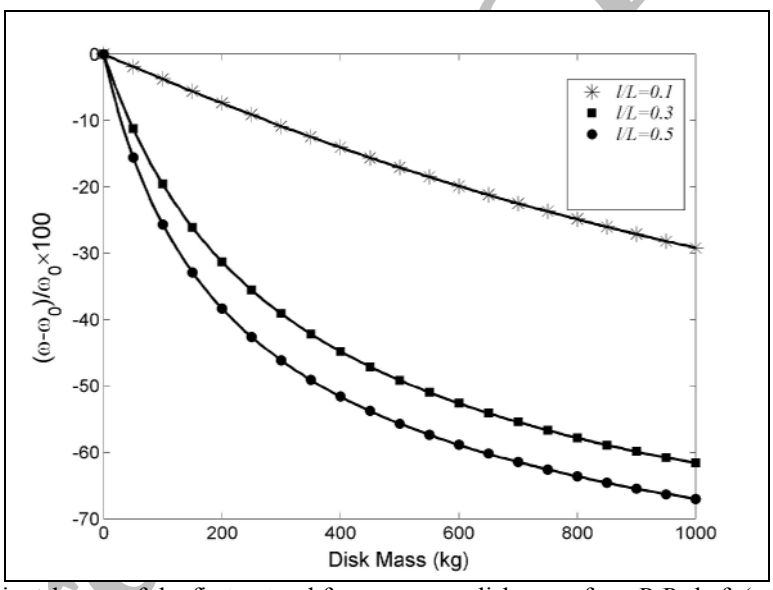

Fig. 6: Relative change of the first natural frequency vs. disk mass for a P-P shaft (with r=0.1 m).

References

1. Meirovitch, L. "Fundamentals of Vibration", McGraw-Hill, New York, 2001.
2. Timoshenko, S., Young, D.H., and Weaver JR., W. "Vibration Problems in Engineering", John Wiley, New York, 1974.
3. Srinivasan, P., "Mechanical Vibration Analysis", McGraw-Hill, New Delhi, 1982.
4. Rao, S.S., "Rotor Dynamics", John Wiley, New York, 1983.
5. L., P.A.A. and Gutierrez, R.H., "Analysis of Vibrating Timoshenko Beams, Using the Method of Differential Quadrature", Shock and Vibration, Vol. 1, No.1, pp. 89–93, 1993.
6. Chakraverty, S., Bhat, R.B., and Stiharu, I., "Recent Research on Vibration of Structures, Using Boundary Characteristic Orthogonal Polynomials in the Rayleigh–ritz Method", The Shock and Vibration Digest, Vol. 31, No. 3, pp. 187–194, 1999.
7. Lee, J. and Schultz, W.W., "Eigenvalue Analysis of Timoshenko Beams and Axisymmetric Mindlin Plates by the Pseudospectral Method", J. Sound and Vibration, Vol. 269, No. 1, pp. 609–621, 2004.
8. Whalley, R., "The Response of Distributed-Lumped Parameter Systems", IMechE, Vol. 202, No. C6, pp. 421-428, 1988.

9. Aleyaasin, M., Ebrahimi, M., and Whalley, R., "Flexural Vibration of Rotating Shafts by Frequency Domain Hybrid Modeling", J. Computers and Structures, Vol. 79, No. 2, pp. 319-331, 2001.
10. Aleyaasin, M., and Ebrahimi, M., "Hybrid Modeling for Analysis and Identification of Rotors", J. Computers Methods in Applied Mech. and Eng., Vol. 182, No. 2, pp. 163-176, 2000.
11. Aleyaasin, M., Ebrahimi, M., and Whalley, R., "Vibration Analysis of Distributed-lumped Rotor Systems", J. Computers Methods in Applied Mech. and Eng., Vol. 189, No. 2, pp. 545-588, 2000.
12. Aleyaasin, M., Ebrahimi, M., and Whalley, R., "Multi-variable Hybrid Models for Rotor-Bearing Systems", J. Sound and Vibration, Vol. 233, No. 5, pp. 835-856, 2000.
13. Farshidianfar, A., Dalir, H. and Shayan Amin, S. "Frequency Investigation of Rotating Rotors Torsional Vibration, Using Hybrid Modeling Technique, Int. Conf. Manufacturing Eng., Amirkabir Univ., Tehran, 2003.
14. Tahani, M., and Soheili, S. "Frequency and Time Response of Rotors Longitudinal Vibration, Using Hybrid Modeling", The 13th Int. Mech. Eng. Conf., Isfahan, 2005.
15. Whalley, R., Bartlett, H., and Ebrahimi, M. "Analytical Solution of Distributed-lumped Parameter Network Models, IMechE, Vol. 211, No. 2, Part I, pp. 203-218, 1997.
16. Farshidianfar, A. and Soheili, S. "Effects of Rotary Inertia and Gyroscopic Momentum on the Flexural Vibration of Rotating Shafts, Using Hybrid Modeling", To be Published in J. Scientia Iranica.

Appendix A

Considering Eq. 26, the main transfer matrix for a shaft with the length *x* could be stated as:

$$[T] = [T(x)][T(0)]^{-1} \tag{A1}$$

Assuming the relation (19a) as the transfer matrix for the distributed element (shaft), in which rotary inertia and shear effects are considered, the main transfer matrix would have the following elements:

$$\begin{aligned}
T_{11} &= \frac{-4(s_{15}+s_{17})s_{22}\omega\sqrt{\rho I s_1}(\rho I\omega^2 - kAG) + s_{21}(s_8+s_{10})}{16(\rho I\omega^2 - kAG)\rho\omega^2 s_1} \\
T_{12} &= \frac{s_{20}\sqrt{Is_3}(-s_{17}+s_{15}) + s_{19}\sqrt{Is_{12}}(s_{10}-s_8)}{2\omega\sqrt{\rho s_1 s_3 s_{12}}} \\
T_{13} &= \frac{kG(s_{17}+s_{15}-s_{10}-s_8)}{2\omega\sqrt{\rho I s_1}} \\
T_{14} &= \frac{s_{13}\sqrt{s_3}(-s_{17}+s_{15}) + s_5\sqrt{s_{12}}(s_{10}-s_8)}{2\omega kAG\sqrt{\rho I s_1 s_3 s_{12}}} \\
T_{21} &= \frac{-4(s_{32}+s_{31})s_{22}\omega\sqrt{\rho I s_1}(\rho I\omega^2 - kAG) + s_{21}(s_{30}+s_{29})}{16(\rho I\omega^2 - kAG)\rho\omega^2 s_1} \\
T_{22} &= \frac{s_{20}\sqrt{Is_3}(-s_{32}+s_{31}) + s_{19}\sqrt{Is_{12}}(s_{30}-s_{29})}{2\omega\sqrt{\rho s_1 s_3 s_{12}}} \\
T_{23} &= \frac{kG(s_{32}+s_{31}-s_{30}-s_{29})}{2\omega\sqrt{\rho I s_1}} \\
T_{24} &= \frac{s_{13}\sqrt{s_3}(-s_{32}+s_{31}) + s_5\sqrt{s_{12}}(s_{30}-s_{29})}{2\omega kAG\sqrt{\rho I s_1 s_3 s_{12}}} \\
T_{31} &= \frac{-4EI(s_{28}+s_{27})s_{22}\omega\sqrt{\rho I s_1}(\rho I\omega^2 - kAG) + EIs_{21}(s_{25}+s_{24})}{16(\rho I\omega^2 - kAG)\rho\omega^2 s_1} \\
T_{32} &= \frac{s_{20}EI\sqrt{Is_3}(-s_{28}+s_{27}) + s_{19}EI\sqrt{Is_{12}}(s_{25}-s_{24})}{2\omega\sqrt{\rho s_1 s_3 s_{12}}} \\
T_{33} &= \frac{EIkG(s_{28}+s_{27}-s_{25}-s_{24})}{2\omega\sqrt{\rho I s_1}} \\
T_{34} &= \frac{EIs_{13}\sqrt{s_3}(-s_{28}+s_{27}) + EIs_5\sqrt{s_{12}}(s_{25}-s_{24})}{2\omega kAG\sqrt{\rho I s_1 s_3 s_{12}}} \\
T_{41} &= \frac{-4kAG(s_{18}+s_{16})s_{22}\omega\sqrt{\rho I s_1}(\rho I\omega^2 - kAG) + kAGs_{21}(s_{11}+s_9)}{16(\rho I\omega^2 - kAG)^2\rho\omega^2 s_1} \\
T_{42} &= \frac{s_{20}kAG\sqrt{Is_3}(-s_{18}+s_{16}) + s_{19}kAG\sqrt{Is_{12}}(s_{11}-s_9)}{2(\rho I\omega^2 - kAG)\omega\sqrt{\rho s_1 s_3 s_{12}}} \\
T_{43} &= \frac{k^2AG^2(s_{18}+s_{16}-s_{11}-s_9)}{2(\rho I\omega^2 - kAG)\omega\sqrt{\rho I s_1}} \\
T_{44} &= \frac{s_{13}\sqrt{s_3}(-s_{18}+s_{16}) + s_5\sqrt{s_{12}}(s_{11}-s_9)}{2(\rho I\omega^2 - kAG)\omega\sqrt{\rho I s_1 s_3 s_{12}}}
\end{aligned} \tag{A2}$$

In which s_1 to s_{32} are the following relations:

$$s_1 = h_1$$
$$s_2 = h_4$$
$$s_3 = \frac{-2h_{13}}{EkG}$$
$$s_4 = h_2$$
$$s_5 = h_3$$
$$s_6 = \frac{\omega}{EkG}\sqrt{\frac{\rho h_1}{I}}$$
$$s_7 = \frac{-2h_{13}}{EkG}$$
$$s_8 = h_{11}$$
$$s_9 = \frac{-Ih_{11}h_{12}\sqrt{h_9}}{4kG}$$
$$s_{10} = h_{10}$$
$$s_{11} = \frac{Ih_{10}h_{12}\sqrt{h_9}}{4kG}$$
$$s_{12} = \frac{-2h_{12}}{EkG}$$
$$s_{13} = h_8$$
$$s_{14} = \frac{-2h_{12}}{EkG}$$
$$s_{15} = h_7$$
$$s_{16} = \frac{-Ih_7h_{13}\sqrt{h_5}}{4kG}$$
$$s_{17} = h_6$$
$$s_{18} = \frac{Ih_6h_{13}\sqrt{h_5}}{4kG}$$
$$s_{19} = h_{13}$$
$$s_{20} = h_{12}$$
$$s_{21} = -4\omega^3(kG-E)(\rho I\omega^2 - kAG)\rho^2 I^2\sqrt{\frac{\rho h_1}{I}} + 16(kAG)(kGE)\rho\omega^2(\rho I\omega^2 - kAG) + 4I\rho^2\omega^4(kG-E)^2(\rho I\omega^2 - kAG)$$
$$s_{22} = -\rho\omega^2(kG-E) - h_4$$
$$s_{23} = \frac{-h_{13}}{2EkG}$$
$$s_{24} = \frac{h_{13}h_{11}h_8}{4Ek^2G^2(\rho I\omega^2 - kAG)}$$
$$s_{25} = \frac{h_{13}h_{10}h_8}{4Ek^2G^2(\rho I\omega^2 - kAG)}$$
$$s_{26} = \frac{-h_{12}}{2EkG}$$
$$s_{27} = \frac{h_{12}h_7h_3}{4Ek^2G^2(\rho I\omega^2 - kAG)}$$
$$s_{28} = \frac{h_{12}h_6h_3}{4Ek^2G^2(\rho I\omega^2 - kAG)}$$
$$s_{29} = \frac{h_{11}h_8\sqrt{h_9}}{4kG(\rho I\omega^2 - kAG)}$$
$$s_{30} = \frac{h_{10}h_8\sqrt{h_9}}{4kG(\rho I\omega^2 - kAG)}$$
$$s_{31} = \frac{h_7h_3\sqrt{h_5}}{4kG(\rho I\omega^2 - kAG)}$$
$$s_{32} = \frac{h_6h_3\sqrt{h_5}}{-4kG(\rho I\omega^2 - kAG)} \quad \text{(A3)}$$

and h_1 to h_{13} can be expressed as:

$$h_1 = r_1$$
$$h_2 = I\omega\sqrt{\frac{\rho r_1}{I}}$$
$$h_3 = 2k^2G^2A - \rho I\omega^2(kG-E) + I\omega\sqrt{\frac{\rho r_1}{I}}$$
$$h_4 = \omega\sqrt{\frac{\rho r_1}{I}}$$
$$h_5 = -\frac{2\rho\omega^2(kG+E) - 2\omega\sqrt{\frac{\rho r_1}{I}}}{kGE}$$
$$h_6 = \exp\left(\frac{x}{2}\sqrt{-\frac{2\rho\omega^2(kG+E) - 2\omega\sqrt{\frac{\rho r_1}{I}}}{kGE}}\right)$$
$$h_7 = \exp\left(-\frac{x}{2}\sqrt{-\frac{2\rho\omega^2(kG+E) - 2\omega\sqrt{\frac{\rho r_1}{I}}}{kGE}}\right)$$
$$h_8 = 2k^2G^2A - \rho I\omega^2(kG-E) - I\omega\sqrt{\frac{\rho r_1}{I}}$$
$$h_9 = -\frac{2\rho\omega^2(kG+E) + 2\omega\sqrt{\frac{\rho r_1}{I}}}{kGE}$$

$$h_{10} = \exp\left(\frac{x}{2}\sqrt{-\frac{2\rho\omega^2(kG+E)+2\omega\sqrt{\frac{\rho r_1}{I}}}{kGE}}\right)$$

$$h_{11} = \exp\left(-\frac{x}{2}\sqrt{-\frac{2\rho\omega^2(kG+E)+2\omega\sqrt{\frac{\rho r_1}{I}}}{kGE}}\right)$$

$$h_{12} = \rho\omega^2(kG+E) - \omega\sqrt{\frac{\rho r_1}{I}}$$

$$h_{13} = \rho\omega^2(kG+E) + \omega\sqrt{\frac{\rho r_1}{I}}$$

(A4)

where:

$$r_1 = \rho I\omega^2(kG-E)^2 + 4AEk^2G^2 \qquad \text{(A5)}$$